JOURNAL OF APPLIED ELECTROCHEMISTRY 14 (1984) 511–520

A study of transport of hydroxyl ion in a chlor-alkali diaphragm

R. R. CHANDRAN, D-T. CHIN

Department of Chemical Engineering, Clarkson University, Potsdam, New York 13676, USA

K. VISWANATHAN

Hooker Development Center, Hooker Chemical Co., PO Box 344, Niagara Falls, New York 14304, USA

Received 4 July 1983; revised 26 August 1983 and 2 November 1983

The loss of hydroxyl ions by diffusion and back migration to the anolyte compartment is the major source of efficiency loss in a chlor-alkali diaphragm cell. The transfer rate of hydroxyl ions across the diaphragm depends on diaphragm properties and electrolyte flow rate inside the diaphragm. This work examines the concentration distribution of hydroxyl ions across the diaphragm in a laboratory cell. A numerical computation is carried out to optimize the diaphragm structure and current density based on the minimum production cost of chlorine. The optimum current density is found to be 50% lower than the present operating current density in the chlor-alkali industry.

Nomenclature

A_P	apparent cross-sectional area of the diaphragm (m^2)
A_T	true cross-sectional area of the pores (m^2)
C_{OH}	concentration of the hydroxyl ion at any point x along the x-direction ($kg\,mol\,m^{-3}$)
C_K	catholyte concentration ($kg\,mol\,m^{-3}$)
C	dimensionless concentration given in Equation 11
C_D	unit diaphragm cost ($\$\,kg^{-1}$)
C_E	unit direct electrical energy cost ($\$\,kg^{-1}$)
C_I	unit specific investment cost ($\$\,kg^{-1}$)
D	diffusion coefficient of the hydroxyl ion ($m^2\,s^{-1}$)
E_0	open circuit voltage (V)
E	total cell voltage (V)
F	Faraday's constants (96 487 C g equiv^{-1})
i_P	apparent current density based on apparent area of the diaphragm, A_P ($A\,m^{-2}$)
i_T	true current density based on true cross-sectional area of the pores, A_T ($A\,m^{-2}$)
I	magnitude of total current through the cell (A)
$(IR)_{BUS}$	voltage drop in the bus-bar (V)
$(IR)_{SOLN}$	voltage drop in the solution (V)
$(IR)_{DIA}$	voltage drop in the diaphragm (V)
N_{OH}	flux of hydroxyl ion ($kg\,mol\,m^{-2}\,s^{-1}$)
K_S	average conductivity of the solution ($ohm^{-1}\,m^{-1}$)
K_1	energy cost ($\$\,kWh^{-1}$)
K_2	capital cost of the electrolyte cell ($\$\,m^{-2}$)
K_3	cost coefficient of diaphragm ($\$\,m^{-2}$)
K_5	unit cost of the raw material ($\$\,kg^{-1}$)
l	effective pore length (m)
l_1	distance between the anode and the cathode (m)
L	life period of the diaphragm (yr)
M_{Cl_2}	molecular weight of chlorine gas (kg)
M_{NaCl}	molecular weight of sodium chloride (kg)
n	number of years of amortization which in principle is given by the life time of the cell (yr)
N_C	total number of cells (dimensionless)
p	production rate of chlorine gas ($kg\,yr^{-1}$)
R	resistance (ohm)
R_0	resistance of the solution (ohm)
S	annual interest rate (%)
U_{OH^-}	mobility of hydroxyl ion

0021–891X/84 $03.00 + .12

	$(kg\,mol\,m^2\,V^{-1}\,C^{-1}\,s^{-1})$
v	electrolyte velocity along the x-direction inside diaphragm $(m\,s^{-1})$
v_S	superficial velocity $(m\,s^{-1})$
V_W	volume of water lost from the catholyte compartment due to evaporation and cathodic reaction $(m^3\,s^{-1})$
x	axial coordinate
Z	valence of hydroxyl ion (kg equiv $kg^{-1}\,mol^{-1}$)
δ	diaphragm thickness (m)
ϵ	porosity (%)
η	current efficiency (dimensionless)
η_a	anodic overpotential (V)
η_c	cathodic overpotential (V)
τ	tortuosity factor (dimensionless)

1. Introduction

The chlor-alkali cell accounts for 75% of the 12 million tons of chlorine produced annually. The diaphragm plays an important role in separating caustic soda from chlorine and is one of the key components of the chlor-alkali cell. There are two incentives to replace the present asbestos separator in a diaphragm cell. The first is the environmental hazard associated with the use of asbestos, and the second is the cost and power reduction consideration. This work is aimed towards an understanding of the structural and transport characteristics of the diaphragm. The results would help in providing information regarding properties of the diaphragm and the change in operating conditions on the existing cells for the new diaphragms.

1.1. *Review of literature*

According to Volkov [1], there was a region inside the diaphragm where catholyte and anolyte neutralized each other under the steady-state operating conditions. At low electrolyte flow rates the neutralization zone shifted towards the anode direction and then into the anode compartment, and lowered the current efficiency. Murray *et al.* [2] studied various processes causing loss of current efficiency in a Hooker cell.

A complete equation for the diffusion and migration of hydroxyl ions had been examined by Ksenzhek *et al.* [3]; their analysis included the change in electrical conductivity and composition of the solution in the diaphragm. These authors also measured the transport number of the hydroxyl ion in a concentrated solution of sodium hydroxide and sodium chloride [4]. Stender *et al.* [5] derived an equation for the calculation of current efficiency as a function of current density, solution-flow velocity and properties of the diaphragm. Verob'eva *et al.* [6] examined the influence of diaphragm thickness (at specified porosity) on the current efficiency of alkali in a laboratory cell with a horizontal diaphragm; the dependence of alkali concentration on diaphragm thickness was presented. Rotinyan *et al.* [7] derived an equation to calculate the alkali concentration under non-steady conditions; they verified their theory experimentally with a horizontal [7–9] and a vertical diaphragm cell [10].

Ksenzhek *et al.* [11–14] made a theoretical consideration of the operation of an electrolytic cell composed of two porous electrodes separated by a porous matrix. Kheifets and Goldberg [15] analysed mixing of electrolysis products, secondary reactions and current efficiency during the electrolysis with a filter-action diaphragm, and presented a modification [16] by taking into account the non-uniform current distribution. The material balance of a diaphragm cell was given by Nagy [17]. Bryson *et al.* [18] attempted to predict the sodium chloride and the hydroxyl ion fluxes using the dilute solution theory.

Kubasov [19] presented a method to estimate the thickness of the diaphragm by considering migration and the diffusion of hydroxide ion. A mathematical model describing the performance of porous separators used in diaphragm chlor-alkali cells was presented by Koh [20]; the diaphragm structure was optimized for a given operating current density. Hine *et al.* [21] found that hydrogen bubbles generated on the cathode screen could penetrate into the asbestos diaphragm and significantly disturb the brine flow. However, if the asbestos was compressed to reduce the hydrogen penetration, the voltage drop across the diaphragm became larger. The permeability of an asbestos diaphragm with and without electric current was studied by Kristalik [22, 23].

1.2. *Aim*

Experimental measurement of concentration

distribution inside the diaphragm has not been previously reported and this work represents the first attempt of this kind. Although a number of optimization calculations had been carried out, they were concentrated on optimizing the diaphragm structure, not the current density. With an increasing necessity to reduce power consumption, this work attempted to optimize the current density and the diaphragm structure simultaneously with a mathematical model.

2. Mathematical modelling

The present analysis is similar to Stender's model [5], but with two important modifications:

1. As distinguished from Stender's model, the actual velocity of electrolyte flow within the pores of the diaphragm is considered.
2. The effect of 'tortuosity' of the diaphragm is taken into account.

Macmullin [24] introduced the tortuosity to describe the amount of winding paths within a separator. He also derived a correlation between the electric resistivity and the properties of the separators, such as hydraulic radius, permeability, etc. The tortuosity can be determined by measuring the resistivity of the electrolyte with and without the separator.

$$\tau(\text{tortuosity}) = R\epsilon/R_0 \tag{1}$$

where R_0 is the resistivity of the solution alone and R the resistivity of the separator soaked with the same electrolyte. Let l represent the actual length of the flow path inside the diaphragm and δ be the thickness of the diaphragm, then

$$\tau = l/\delta \tag{2}$$

The porosity of a diaphragm is defined as the ratio of the pore volume to the volume of the diaphragm. It may be related to the tortuosity by

$$\epsilon = A_T l/A_P\delta = (A_T/A_P)\tau \tag{3}$$

where A_T is the true cross-sectional area of the pores perpendicular to the direction of flow and A_P is the apparent cross-sectional area of the diaphragm which is equal to the apparent area of the electrodes in the chlor-alkali cell.

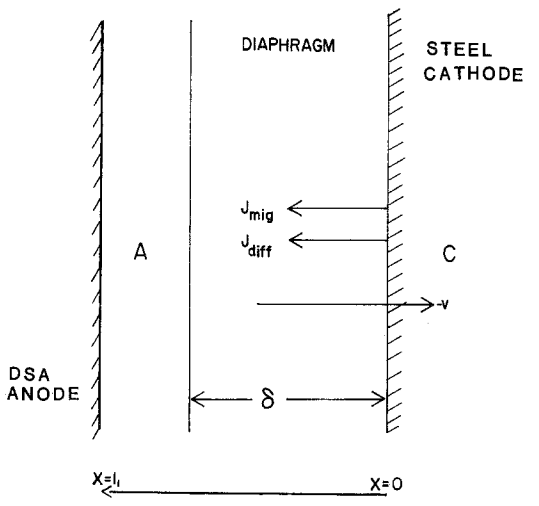

Fig. 1. Scheme of flow distribution in the diaphragm. A-anolyte; C-catholyte.

2.1. *Transport of hydroxyl ion across the diaphragm*

The direction of mass flux of hydroxyl ion through the diaphragm is shown schematically in Fig. 1. The net flux of OH^- ions in an arbitrary section of the diaphragm may be given by

$$N_{OH} = U_{OH}FC_{OH}(d\phi/dx) - D_{OH}(dC_{OH}/dx) + vC_{OH} \tag{4}$$

where C_{OH} is the alkali concentration and X is the distance from the catholyte compartment along the tortuous path in the porous diaphragm. The electrolyte velocity, v, and the flux, N, are based on the true cross-sectional area of the pores; their values will be positive if they are along the X-direction.

The potential gradient across the diaphragm may be given by Ohm's law

$$d\phi/dx = -i_T/k \tag{5}$$

where i_T is the true current density based on the cross-sectional area of the pores A_T. The true current density, i_T, is related to the apparent current density, i_P, by

$$i_T = i_P(A_P/A_T) = i_P\tau/\epsilon \tag{6}$$

The actual velocity, v, inside the pores can be expressed in terms of a superficial velocity, v_S, as

$$v = v_S(\tau/\epsilon) \tag{7}$$

Substituting Equations 5–7 into Equation 4, one has

$$N_{OH} = -D_{OH}(dC_{OH}/dx) + (\alpha\tau/\epsilon)C_{OH} \quad (8)$$

The quantity, α, in Equation 8 is a vectorial sum of the migrational velocity and the convective velocity of OH^- ion:

$$\alpha = -U_{OH}Fi_P/k + v_S \quad (9)$$

Knowing that $C_{OH} = C_K$ at $x = 0$. Equation 8 may be integrated to give

$$C^* = e^{NX^*}e^{-N}/(e^{-N} - 1) - 1/(e^{-N} - 1) \quad (10)$$

where

$$C^* = C_{OH}/C_K \quad (11)$$

$$X^* = x/l \quad (12)$$

$$N = \alpha\delta\tau^2/D\epsilon \quad (13)$$

The quantity N represents the ratio of the sum of the convective and migrational fluxes to the diffusional flux of OH^- ion; its physical significance is similar to the Sherwood number in transport problems.

The flux, N_{OH}, represents the amount of sodium hydroxide (alkali) entering the anode compartment and is irretrievably lost. Thus the current efficiency in the NaOH production, η, may be related to N_{OH} by

$$N_{OH} = (|i_P|/F)(\tau/\epsilon)(1 - \eta) \quad (14)$$

where $|i_P|/F$ represents the rate of alkali formed at the cathode. Combining Equations 10 and 14, the current efficiency of a diaphragm chlor-alkali cell may be related to the hydroxyl ion concentration in the catholyte by the expression:

$$\eta = 1 + (F\alpha C_K/|i_P|)\,[e^N/(1 - e^N)] \quad (15)$$

2.2. *Optimization of diaphragm characteristics and operating current density*

The unit production cost of chlorine can be expressed as:

$$\begin{aligned}\text{unit cost} &= (\text{total production cost})/\\ &\quad (\text{kg of } Cl_2 \text{ produced})\\ &= (\text{cost of direct electrical energy})\\ &\quad + (\text{specific investment})\\ &\quad + (\text{diaphragm cost})\\ &\quad + (\text{cost of raw materials})\\ &\quad + (\text{other costs}) \quad (16)\end{aligned}$$

The unit direct electrical energy cost, C_E \$ $(\text{kg } Cl_2)^{-1}$, can be obtained in terms of Faraday's law and the operating cell voltage as

$$C_E = 2K_1FE/(M_{Cl_2}\eta\,3600) \quad (17)$$

where K_1 and M_{Cl_2} are the cost coefficient of electrical energy in \$ kWh^{-1}, and molecular weight of Cl_2 respectively. The operating cell voltage, E, is given by the expression:

$$E = E_0 + \eta_a - \eta_c + (IR)_{BUS} + (IR)_{SOLN} + (IR)_{DIA} \quad (18)$$

Here, E_0 is the open circuit cell voltage which varies from 2.19 V at 25° C to 2.13 V at 90° C in typical industrial chlor-alkali cells [28]. The voltage drop in the bus-bar, $(IR)_{BUS}$, may be taken to be equal to 250 mV at 150 kA load. The anodic and the cathodic polarization curves have been experimentally determined in this work. The anodic overpotential, η_a on a dimensionally stable anode (DSA) in 5M NaCl (pH = 3.5) at 95°C may be given by the expression:

$$\eta_a(\text{mv}) = 27.7 \log(0.1|i_P|) - 2.5 \quad (19)$$

The cathodic overpotential on steel in 15% NaOH + 17% NaCl at 95° C may be given by the expression:

$$\eta_c(\text{mv}) = -121.9 \log(0.1|i_P|) + 87.5 \quad (20)$$

The voltage drop in the solution between anode and the diaphragm surface facing the anode is obtained by the expression:

$$(IR)_{SOLN} = |i_P|(l_1 - \delta)/K_S \quad (21)$$

where l_1 is the distance between the anode and the cathode and K_S is the conductivity of the anolyte. The last term in the Equation 18 represents the potential drop across the diaphragm and it can be expressed in the following form:

$$(IR)_{DIA} = (|i_P|/K)(\tau/\epsilon)\delta\tau \quad (22)$$

The average solution conductivity, K, in Equation 22 may be calculated assuming an average composition within the diaphragm to be

1. 75% anolyte + 25% catholyte
2. 80% anolyte + 15% catholyte
3. 85% anolyte + 15% catholyte.

The difference in these assumptions are small, and the values fall within ± 2%. However, when conductivity is calculated assuming an average composition within the diaphragm to be of 100% anolyte, the conductivity is 7% smaller. In this work an average composition of 75% anolyte + 25% catholyte is assumed for numerical calculations.

The unit specific investment cost can be calculated by using Formula 23

$$C_I[\$\,(\mathrm{kg\,Cl_2})^{-1}] \quad (23)$$
$$= K_2|I/i_P|N_C\{(S+1)^nS/[(S+1)^n-1]\}/p$$

Here, S, n, N_C, I and K_2 represent the interest rate, number of years of amortization, total number of cells, the total current and the capital cost of the electrolytic cell ($\$\,m^{-2}$), respectively. The annual production rate of chlorine, p, can be calculated using Faraday's law:

$$p(\mathrm{kg\,yr^{-1}}) = (N_C)(I)M_{Cl_2}\eta(86\,400 \times 365)/2F \quad (24)$$

The unit diaphragm cost, C_D $[\$(\mathrm{kg\,Cl_2})^{-1}]$ can be given by the expression:

$$C_D = K_3|I/i_P|N_C/L_Dp \quad (25)$$

where K_3 is the cost coefficient of the diaphragm in $\$\,m^{-2}$. It is assumed that the diaphragm has a useful life of L years. In the case of asbestos a constant cost of $0.153\,\$\,(\mathrm{kg\,Cl_2})^{-1}$ is used in the present calculation.

The main raw material for the process is sodium chloride whose cost coefficient may be represented by K_5 in $\$\,(\mathrm{kg\,NaCl})^{-1}$. The unit raw material cost, C_R, can be calculated from the equation:

$$C_R[\$\,(\mathrm{kg\,Cl_2})^{-1}] = 2M_{NaCl}K_5/M_{Cl_2} \quad (26)$$

The other costs including the overhead, labour and maintenance costs, are taken to be constant, K_6 $[\$(\mathrm{kg\,Cl_2})^{-1}]$. The unit cost mentioned hereafter will not include this constant, K_6, as it is not available readily. This will not hinder the optimization calculation.

Substituting Equations 17–26 into Equation 16 the objective function in the present analysis can be written in the following form:

$$\text{unit cost } [\$\,(\mathrm{kg\,Cl_2})^{-1}] = 2K_1FE/(M_{Cl_2}\eta 3600)$$
$$+ K_2|I/i_P|N_C\{(S+1)^nS/[(S+1)^n-1]\}/p$$
$$+ K_3|I/i_P|(N_C)/L_Dp + 2M_{NaCl}K_5/M_{Cl_2} \quad (27)$$

With the help of Equation 15 for current efficiency and Equation 18 for cell voltage, it is found that there are two important variables which characterize the objective function. They are:

1. magnitude of apparent current density, $|i_P|$
2. $N = \alpha\delta\tau^2/D\epsilon$.

A material balance of hydroxyl ion for unit cross-sectional area of the diaphragm reveals that the relationship between the electrolyte flow rate and the apparent current density is an implicit relationship, and is given by the equation

$$\alpha/(1-e^{-N}) = |i_P|/F\alpha C_K - U_{OH}F|i_P|/K + V_W/A_P \quad (28)$$

where V_W is the amount of water lost in the catholyte compartment due to evaporation and the decomposition during the course of cathodic reactions. The total water loss may be taken to be $40\,\mathrm{kg\,H_2O\,(kg\,H_2)^{-1}}$. Two important parameters are the current density and the catholyte alkali concentration. If the current density is increased then in order to keep the concentration of the alkali at a constant value in the catholyte, the feed rate should be increased correspondingly. In view of this, the quantity N is not an independent variable, as it depends on the current density, i_P, as shown by Equation 28. Hence, the following two quantities are selected as the variables to be optimized:

1. magnitude of apparent current density, $|i_P|$
2. diaphragm structural property, $\delta_{eff} = \delta\tau^2/\epsilon$

which can be regarded as the effective diffusional length for OH^- ions inside the diaphragm.

Using a Hookes and Jeeves direct search method [25, 26], a computer program has been prepared to locate the optimal values of $|i_P|$ and δ_{eff} to minimize the unit cost, Equation 16. The input parameters and transport properties for the numerical calculation are given in Table 1.

3. Experimental details

Experiments were carried out with a porous packed bed of glass beads to simulate the per-

Table 1. Numerical values of various constants used in the calculation

Open circuit voltage, E_0	2.13 V at 90° C
Faraday's constant, F	96 487 C g equiv^{-1}
Total current load, I	150 kA
Voltage drop in the bus-bar, $(IR)_{BUS}$	0.25 V
Number of cells, N_C	200
Energy cost, K_1	0.04 \$ kWh^{-1}
Capital cost of the cell, K_2	400 \$ m^{-2}
Annual interest rate, S	15%
Unit cost of the raw material, K_5	0.015 \$ kg^{-1} of NaCl
Mobility of hydroxyl ion, U_{OH} at 90° C	1.553 X 10^{-15} m kg mol C^{-1} s^{-1}
Diffusion coefficient of hydroxyl ion, D_{OH} at 90° C	4.687E-09 m^2 s^{-1}
Conductivity of the anolyte, K_S at 90° C	58.99 ohm^{-1} m^{-1}
Average conductivity of the solution within the diaphragm, K, at 90° C	65.6 ohm^{-1} m^{-1}

formance of a diaphragm. They were used to measure the concentration distribution of hydroxyl ions within the diaphragm. A schematic diagram of the cell is shown in Fig. 2. The cell consisted of three separate sections. They were: (a) a diaphragm section made of Teflon, (b) an anolyte and (c) a catholyte compartment both made of pyrex glass.

The packing materials had to be selected with care. The diaphragm made of a porous packed bed should be able to give sufficient pressure drop so that there will be sufficient anolyte head height to keep the electrolyte flow uniform across the diaphragm. The size of the particles was critical in getting good performance. The material was also important because of the corrosive environment. Various packing materials, including a glass, ceramic, Teflon and zirconium oxide, were tried. It was found that glass beads of 100 microns, pretreated with NaOH to form a protective oxide coating, performed well. The glass beads were soaked in NaOH for a day before using and packed between two Teflon filter papers which had been pretreated with a wetting agent ('Zonyl' FSN fluorosurfactant obtained from E. I. Dupont De Nemours & Co.). The filter paper was 0.001 27 cm thick and had a pore size of approximately 30 microns. The filter paper was further supported by two circular polypropylene meshes

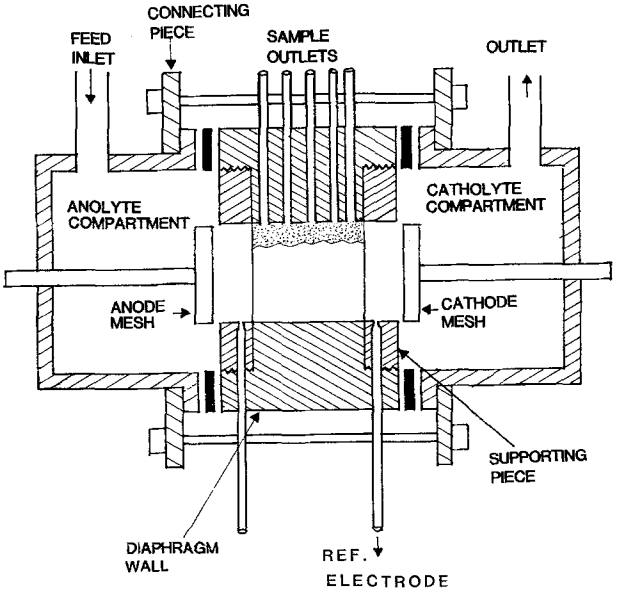

Fig. 2. Schematic diagram of the experimental cell.

to avoid sagging and shape change. The packed section was 2.86 cm in length with an apparent cross-sectional area of 8.58 cm^2, and it had a value of 4.0 for τ^2/ϵ. The filter paper, glass beads and the polypropylene mesh were held in place by two supporting pieces threaded onto the diaphragm section as shown in Fig. 2.

Two capillary openings were provided on the bottom wall of the diaphragm section with one on each side of the packed bed. The capillary openings were connected to the Teflon PFA tubings, 0.1587 cm ID x 0.3175 cm OD. A platinum wire was inserted into the tubing and used as the reference electrode. With this arrangement, the potential drop across the diaphragm could be measured.

Provisions were made to draw liquid samples at various locations on the diaphragm sections to measure the concentration of hydroxyl ion. A Teflon PFA minibore tubing of 0.0305 cm ID x 0.0762 cm OD was used for this purpose by inserting it into the porous packed bed. The liquid sample in the amount 50–100 μl was drawn out using a microsyringe. The concentration of OH^- ion was measured by titration with standard 0.1N HCl acid solution using a microburette with an accuracy of 10 μl.

A dimensionally stable anode (DSA) fabricated from titanium coated with ruthenium and titanium oxide as active catalyst was used. The cathode was made from a steel mesh. The apparent area of the electrode was the same as the diaphragm.

The brine solution of concentration 290 g l^{-1}, made from analytical grade sodium chloride (Baker analysed reagent) was pumped from a storage tank with a Masterflux tubing pump. During the electrolysis chlorine gas was absorbed in NaOH solution. A DC power supply (Hewlett-Packard, Model 6274 B) was used to supply a constant DC current. A two channel recorder (Cole-Parmer, Model 8376-30) was used to record cell voltage as well as the diaphragm voltage drop. The concentration of NaOH produced was in the range of 3–4M. The operation took a day to reach the steady-state NaOH concentration and the current efficiency remained constant afterwards. To measure the current efficiency, samples of catholyte NaOH were collected and titrated against 1N HCl. The current efficiency was calculated by knowing the experimental production rate and the theoretical amount according to Faraday's law.

4. Results and discussion

4.1. *Concentration of hydroxyl ion within the diaphragm*

Fig. 3 shows the theoretical concentration distribution of OH^- ions calculated from Equation 10 for various values of N, which is the controlling factor in the cell operation. When N is negative (i.e. $\alpha < 0$) the concentration gradient decreases in magnitude towards the anode side and when N is positive (i.e. $\alpha > 0$) the curve becomes convex. In reality, the values of N should be less than zero throughout the diaphragm for effective separation. The more negative the values of N, the more concave is the drop of OH^- concentration within the diaphragm. One way of getting higher negative values of N is by increasing the electrolyte flow rate to make α more negative. This pushes the back-migrating OH^- ions towards the cathode compartment, and hence improves the current efficiency.

Fig. 4 shows the results of experimental con-

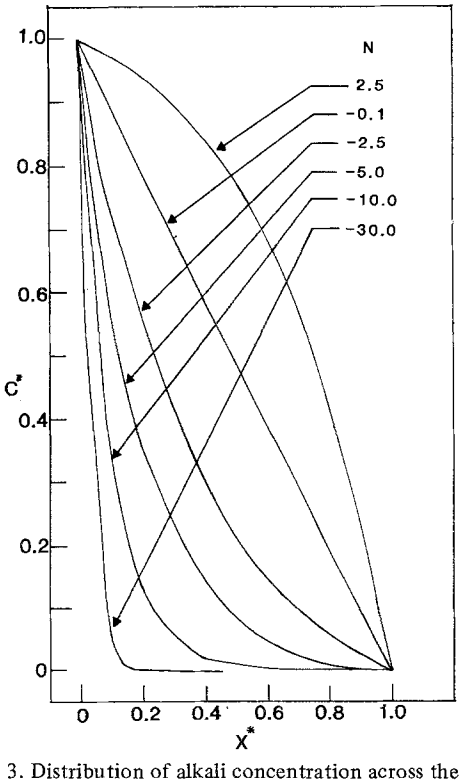

Fig. 3. Distribution of alkali concentration across the diaphragm at different N.

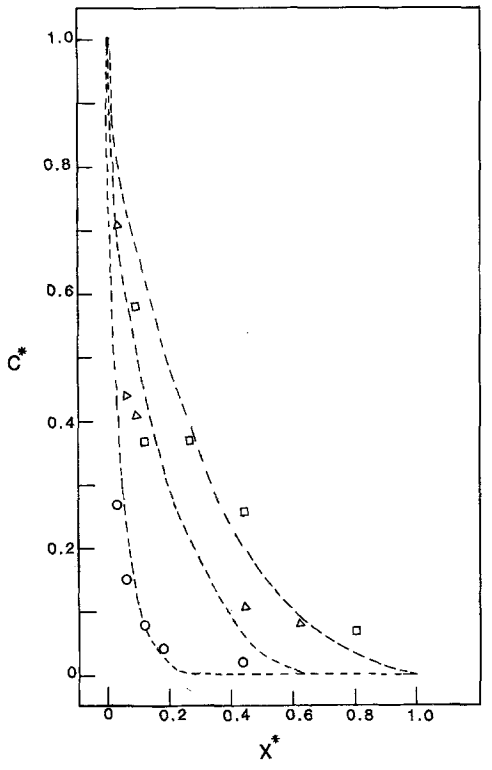

Fig. 4. Distribution of alkali concentration across the diaphragm measured in a laboratory cell at different current density and flow rate. ○ $I = 2$A; $\eta = 90\%$; flow rate = 0.397×10^6 m^3 s^{-1}; $C_K = 3.19$ kg mol m^{-3}; $N = -23.9$. △ $I = 2$A; $\eta = 80\%$; flow rate = 0.256×10^6 m^3 s^{-1}; $C_K = 3.85$; $N = -7.25$. □ $I = 1.5$ A; $\eta = 54\%$; flow rate = 0.141×10^6 m^3; $N = -3.50$.

centration measurements obtained at various current densities and flow rates. For a constant cell current a reduction in flow rate increased the catholyte hydroxyl concentration and decreased the current efficiency. The concentration profile qualitatively behaves according to Equation 10. The data were obtained when the cell was operated at a temperature of 40° C.

When both the anolyte and the catholyte compartments were kept at 90° C, the cell voltage started at an initial value and kept increasing after some time. It was found that the heat generated inside the diaphragm due to *IR* drop caused the temperature to rise. Once the liquid reached the boiling point the vaporization of liquid caused the cell voltage to rise continuously, and the experiment had to be terminated when the cell voltage reached the maximal output of the power supply. This added to the problem of non-uniform temperature inside the diaphragm. It is believed that this might have caused the scattering of the data obtained in the present measurements. The diaphragm voltage drop was always found to be less than the theoretical prediction using Equation 22, assuming the temperature inside the diaphragm to be the same as that in the anolyte or catholyte compartment. This voltage measurement revealed that the temperature inside the diaphragm was higher than that inside the anodic and the cathodic compartments. Since the temperature inside the diaphragm was not known exactly, the experimental points could not be compared quantitatively with Equation 10. Hence, a curve fit was made and best values of N were obtained as shown in Fig. 4.

The deviation of experimental values from the curve-fitted profile was small at high N values. However, the deviation became larger at small values of N, and this was probably caused by the non-uniform velocity profile at a small electrolyte flow rate. When the flow rate became smaller the pressure head in the anolyte compartment decreased and hence the velocity deviated from uniformity.

4.2. *Numerical optimization*

Fig. 5 shows the energy consumption calculated

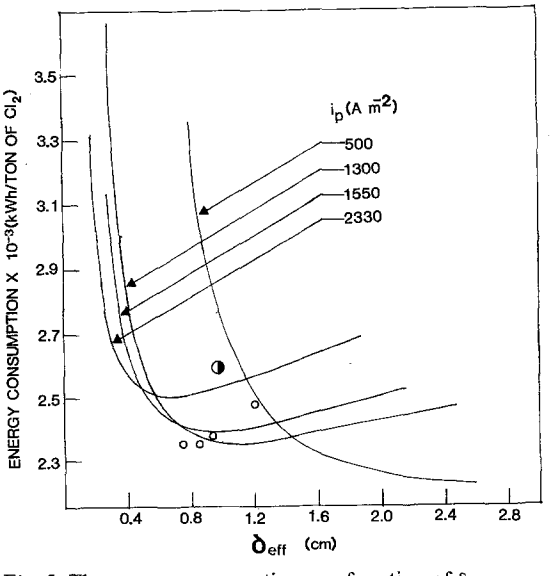

Fig. 5. The energy consumption as a function of δ_{eff}. ◑ indicates the experimental results obtained in a laboratory cell at a current density of 0.233 A cm^{-2}. ○ indicates Koh's experimental results with asbestos at a current density of 0.13 A cm^{-2}.

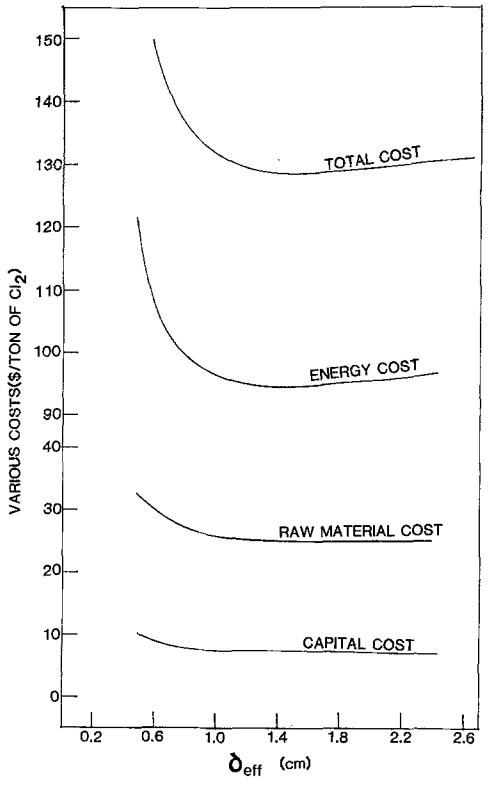

Fig. 6. The objective function vs δ_{eff} at optimum current density. $|i_P|$ (optimum) = 1160 A m^{-2}; C_K = 150 kg m^{-3}.

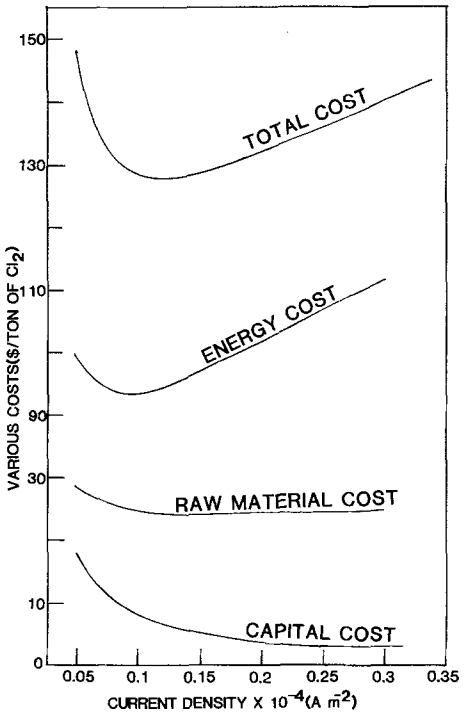

Fig. 7. The objective function vs the current density at optimum δ_{eff}. δ_{eff} (optimum) = 1.54; C_K = 150 kg m^{-3}.

from the following expression

$$\text{energy consumption [kWh (ton Cl}_2\text{)}^{-1}] = ZFE/(N_C)M_{Cl_2}\eta 3.6 \quad (29)$$

as a function of effective diaphragm thickness, δ_{eff}, for various current densities. The figure also shows the energy consumption for a laboratory cell with the same diaphragm for a current density of 0.233 A cm^{-2}. As can be seen, the agreement is within ± 2%. The figure also shows Koh's experimental results on asbestos [27], which compare favourably with the model (± 4% agreement). There exists a minimum energy consumption in all the cases.

The optimum $|i_P|$ and δ_{eff} obtained from the computer optimization are 0.116 A cm^{-2} and 1.54 cm. Fig. 6 shows the variation of various costs with δ_{eff} at optimum current density and Fig. 7 shows the variation with current density at optimum δ_{eff}. From both figures, it is clear that the total cost is a strong function of the current density. The optimum current density is found to be 50% lower than the present operating conditions, which is about 0.23 A cm^{-2}.

4.3. *Sensitivity tests*

With a rapid increase in energy cost, it is important to know what effect the energy cost will have on the optimum parameters. Table 2 shows the effect of energy cost on δ_{eff} at the optimum current density. As one can see, δ_{eff} (optimum) does not change. However, as expected, the total cost

Table 2. Effect of energy cost on optimal $\delta_{eff}|i_P|(opt)$ = 1160 *A m*$^{-2}$; C = 150 *kg m*$^{-3}$; T = 90° *C; basis of cost = year* 1982

Energy cost ($ kWh^{-1})	*Optimal* δ_{eff} (cm)	*Total cost in* $ (ton Cl_2 produced)$^{-1}$
0.04	1.54	129
0.05	1.53	152
0.06	1.53	176
0.07	1.51	199

Table 3. Effect of diaphragm property, τ^2/ϵ on optimum thickness. $|i_P|(opt) = 1160\,A\,m^{-2}$; $C = 150\,kg\,m^{-3}$; $T = 90°\,C$; *basis of cost = year of* 1982

τ^2/ϵ	δ_{eff} (cm)	δ (cm)	*Total cost* \$ (ton of Cl_2)$^{-1}$
3.05	1.54	0.50	129
4.00	1.51	0.38	130
5.00	1.48	0.30	130

increases with increasing energy cost. Table 3 shows the effect of diaphragm property, δ_{eff}, on the optimum diaphragm thickness. The results indicate that with an increase in τ^2/ϵ value, the thickness of the diaphragm can be reduced.

5. Conclusion

A mathematical model has been presented for the transport of OH^- ion and the optimization of the structure and current density within a chlor-alkali diaphragm. The concentration distribution of OH^- within the diaphragm was experimentally measured with a laboratory cell using packed glass beads as the diaphragm. The experimental profile showed a qualitative agreement with the theoretical predictions. The optimum current density was found to be about 50% less than the present operating conditions of the chlor-alkali industry. The optimal value for the diaphragm structure, $\delta_{eff} = \delta\tau^2/\epsilon$ was found to be approximately equal to 1.5. The unit chlorine production cost was not a strong function of the diaphragm property in the range of $1.0 < \delta_{eff} < 2.2$. However, an increase in the tortuosity-to-porosity ratio, τ^2/ϵ, would result in a decrease in the optimum thickness of the diaphragm.

Acknowledgement

The authors would like to thank A. C. Schulz, E. H. Cook and C. A. Lazarz of Hooker Chemicals and Plastics Corporation, Niagara Falls, New York, for their help in the initiation of this investigation. One of the authors, R. R. Chandran, was partially supported by a Hooker Research Fellowship.

References

[1] G. I. Volkov, *Electrokhim.* **14** (1978) 1377.
[2] R. I. Murray and M. S. Kircher, *Trans. Electrochem. Soc.* **86** (1944) 83.
[3] O. S. Ksenzhek and V. M. Serebritskii, *Electrokhim.* **4** (1968) 1439.
[4] V. M. Serebritskii and O. S. Ksenzhek, *Zh. Prikl. Khim.* **43** (1970) 75.
[5] V. V. Stender, O. S. Ksenzhek and V. N. Lazarev, *ibid.* **40** (1967) 1293.
[6] V. B. Verob'eva and V. L. Kubarov, *Electrokhim.* **14** (1978) 943.
[7] A. L. Rotinyan, I. S. Keifets and P. B. Zhivotinskii, *Zh. Prikl. Khim.* **38** (1965) 78.
[8] A. L. Rotinyan and I. S. Stepanyan, *ibid.* **47** (1974) 356.
[9] *Idem, ibid.* **45** (1972) 1548.
[10] I. S. Stepanyan, L. A. Dasoyan, Zh. S. Ter-Kazaryan, V. G. Egishyan and A. V. Arutyunyan, *Electrokhim.* **9** (1973) 845.
[11] O. S. Ksenzhek, E. A. Kalinwskii, B. G. Grishaenkov, E. M. Shembel and V. A. Peredkov, *Electrokhim.* **9** (1973) 358.
[12] *Idem, ibid.* **9** (1973) 641.
[13] O. S. Ksenzhek, E. A. Kalinovskii and E. M. Shembel, *ibid.* **10** (1973) 152.
[14] O. S. Ksenzhek, E. A. Kalinovskii, E. M. Shembel, Y. K. Rossinskii and V. A. Shustov, *ibid.* **12** (1974) 387.
[15] L. I. Kheifets and A. B. Goldberg, *ibid.* **12** (1976) 1673.
[16] *Idem, ibid.* **13** (1977) 149.
[17] Z. Nagy, *J. Electrochem. Soc.* **124** (1977) 91.
[18] A. W. Bryson, P. G. Cook and M. G. Lawrence, *Chem. Eng. Commun.* **3** (1979) 53.
[19] V. L. Kubasov, *Electrokhim.* **12** (1976) 76.
[20] W. H. Koh, *AIChE Symposium Series No. 204* **77** (1981) 213.
[21] F. Hine, M. Yasuda and T. Tanaka, *Electrochim. Acta* **22** (1977) 429.
[22] L. I. Krishtalik, *Zh. Prokl. Khim.* **36** (1963) 1776.
[23] *Idem, ibid.* **36** (1963) 958.
[24] R. B. Macmullin and G. A. Muccini, *AIChE Journal* **2** (1956) 393.
[25] R. Hooke and T. A. Jeeves, *J. Assoc. Computer Machines* **8** (1961) 212.
[26] K. L. Hsueh, D-T. Chin, J. McBreen and S. Srinivasan, *J. Appl. Electrochem.* **11** (1981) 503.
[27] W. H. Koh, Abstract No. 391. Paper presented at the 157th Meeting of the Electrochemical Society, St. Louis, Missouri, 11 May, 1980.
[28] R. C. Weast, 'Handbook of Chemistry and Physics', 52nd edition. The Chemical Rubber Co., Cleveland, Ohio (1971–72).